The Physical Parameters of the Low-Mass triple system LHS1070 from spectral synthesis analysis

A.S. Rajpurohit[1], C.Reylé[1], M.Schultheis[1], C. Leinert[2], F.Allard[3]
[1]Université de France Comté, Institut UTINAM CNRS 6213, Observatoire des Sciences de l'Univers THETA de Franche-Comté, Observatoire de Besançon
[2]Max-Planck-Institut for Astronomie, Konigstuhl,Heidelberg
[3]ENS, Centre de Recherche Astronomique de Lyon

Introduction

M dwarfs are the most numerous stars in our galaxy which makes them an important probe for our galaxy to understand their kinematics and atmospheric properties. The distribution of energy in these late type stars is governed by various molecular absorption bands like TiO, CaH, VO etc which complicates the understanding of their physical properties. Our understanding of these low mass star completely relies upon the model atmosphere. For complete and proper understanding of their physical parameter an accurate atmospheric model is the key . **LHS1070** is a triple system located at a distance of 7.72 ±0.15 pc from the sun (**Seifahrt et al.,2008,A&A,484,429).** It is a nearby 15th magnitude star with high proper motion (**Leinert et al. 2001,A&A,367,183**). This system is thought to be a member of the old disk population with an age of several Gigayerars. This system is very important to study as it helps to determine the dynamical mass of the lower end of the main-sequence. To determine the physical parameters Teff, radius and log(g) we did the comparison of the well calibrated HST/NICMOS spectra for all the component in the optical and in IR with synthetic spectra computed from recent cool stars atmosphere models.

Physical Parameter determination

The grid of synthetic spectra is computed with the recent **BT-Settl Model** (available online) ranging from T = 2000K to 4000K in 100K steps with gravity ranging from log g = 4.0 to 5.5 in a step of 0.5 dex at solar metallicity. The physical parameters of the three component A,B,C such as effective temperature, gravity and radius have been calculated using chi2 minimization technique in an automatic interactive way. Fig. 1 and Fig. 2 in the right panel shows the chi2 maps for the component A and B. Fig. 3 and Fig. 4 shows the physically acceptable solution for the component A and B based on chi2 values in the optical and in near-IR. Similar studies has been done for the component C in optical and in IR. The obtained Teff, log(g) and radius for component A is 2900K,5.5,0.132$R_\odot$ for component B is 2500K,5.5,0.102$R_\odot$ and for component C is 2400K,5.5,0.098R⊙. From the chi2 values and by visual inspection the uncertainty in the obtained values of the Teff is ± 100k and in radius is ± 0.015 $R_\odot$.

Atmospheric Model

The advancement of the model atmosphere of the cool stars is based on the molecular opacities data base and the details knowledge of the atoms and molecule which prevent straightforward derivation of effective temperature and metallicities from the line ratios. The recent **BT-Settl model** (**Allard et al.,2010arXive1011.5405A**) uses the model atmosphere code **PHOENIX** where important molecular opacities and chemical equilibrium calculation are treated and which is based on the 2-D hydrodynamic simulation including a description of dust grain formation from **Freytag et al.,2010,A&A,531,A19** . We have done the comparison of spectra computed from BT-Settl model and the available MARCS model (**Gustafsson,B, et al.,2008,A&A,486,951**) with that of all the component using the same procedure as describe above and found that there is a difference of 100K in effective temperature between the two models. Fig. 5 and Fig. 6 shows both models for the component A and B. Both model give q quite good overall agreement, although differences are found in some regions, probably due to different molecular opacities used. This study can help to improve models.

We thanks N.Ryde for providing us with the MARCS spectra

Contact: arvind@obs-besancon.fr

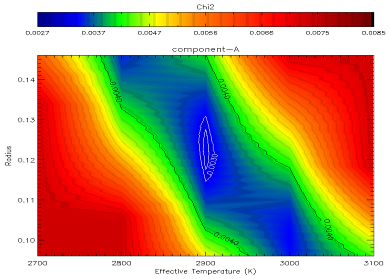

Fig. 1 Chi2 Plot for the component A.

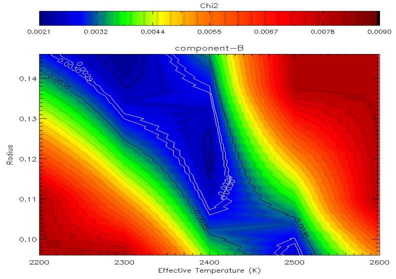

Fig. 2 Chi2 Plot for the component B

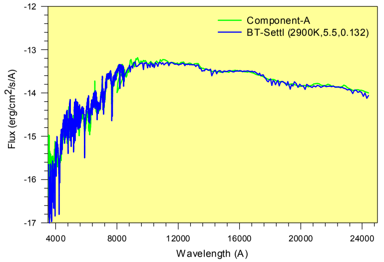

Fig. 3 Comparison of the observed spectra of component A in optical and in near-IR with the synthetic spectra.

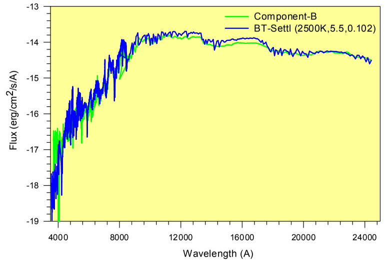

Fig. 4 Comparison of the observed spectra of component B in optical and in near-IR with the synthetic spectra .

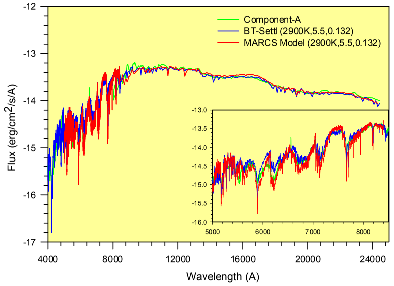

Fig. 5 Comparison of the observed spectra of component A in optical and in near-IR with the BT-Settl and MARCS model

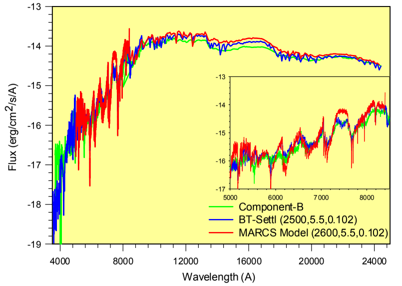

Fig. 6 Comparison of the observed spectra of component B in optical and in near-IR with the BT-Settl and MARCS model